Mean Drift Loads on Arrays of Free Floating OWC Devices Consisting of Concentric Cylinders

by Dimitrios N. Konispoliatis and Spyros A. Mavrakos*

National Technical University of Athens, School of Naval Architecture and Marine Engineering
9 Heroon Polytechniou Ave, GR 157-73, Athens, Greece
E-mail: *mavrakos@naval.ntua.gr ; dconispoliatis@yahoo.gr*

1. Introduction

In this study numerical and experimental results concerning the mean drift loads exerted on an array of free floating OWC's devices are presented. The work is a follow up of the corresponding work presented in the last year Workshop (see [1]) by accounting now for devices that consist of free floating concentric cylinders which are exposed to the action of regular plane waves propagating in finite depth waters. The numerical results have been obtained using both the method of direct integration of the hydrodynamic pressure on the instantaneous wetted surface of the body (see [2], [3]), as well as the momentum conservation principle (see [4], [5], [6], [7]) within properly defined fluid control volumes that surround each OWC device in the array. The required first–order velocity potentials around each body of the multi–body configuration have been obtained analytically by solving the corresponding diffraction, motion– and pressure–dependent–radiation problems for the hydrodynamically interacting OWC's. The hydrodynamic interaction effects are evaluated using the single OWC's hydrodynamic characteristics and the physical idea of multiple scattering (see [8], [9]). The numerical predictions are compared between each other; whereas for some configurations they are supplemented by experimental results obtained during an experimental campaign conducted in CEHIPAR research institution (see [10]).

2. Methodology

We consider a group of *N* vertical axisymmetric OWC devices, either floating independently or as a unit.The geometric configuration of each device consists of an exterior partially immersed toroidal oscillating chamber of finite volume supplemented by a concentric interior piston– like truncated cylinder (Figs. 1, 2). Small amplitude, inviscid, incompressible and irrotational flow is assumed, so that linear potential theory can be employed. A number of *N* local cylindrical co–ordinate systems $\left(r_q,\theta_q,z_q\right)$, are defined with origins on the sea bottom and their vertical axes pointing upwards and coinciding with the vertical axis of symmetry of the *q* device.

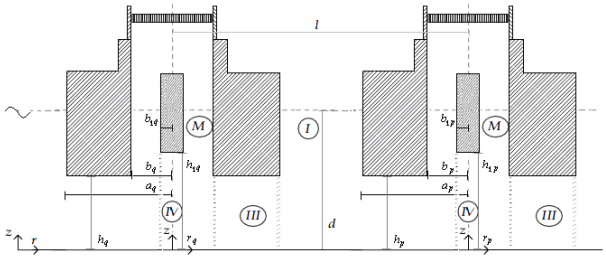

Fig.1 Schematic representation of an array of OWC devices consisting of a concentric truncated cylinder placed in a row

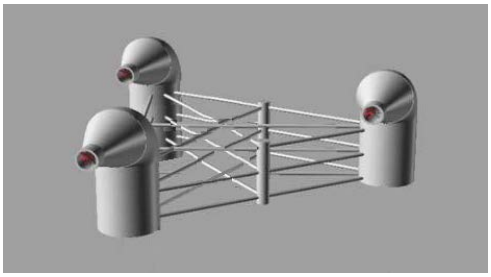

Fig. 2 Group of *N* identical OWC devices connected as a unit, forming a platform

The fluid flow around the *q*=1,2,…,*N* device expressed in its own co-ordinate system can be described by the potential function: $\Phi^q\left(r_q,\theta_q,z;t\right)=\mathrm{Re}\left\{\phi^q\left(r_q,\theta_q,z\right)\cdot e^{-i\omega t}\right\}$, which can be decomposed into three terms; the diffraction potential, ϕ_D^q (includes incident and scattered components); the motion–radiation potential, ϕ_j^{qp}, induced around the device *q* due to the forced oscillation of the device *p* in the *j*th direction with unit velocity amplitude, $\dot{x}_j^p=\mathrm{Re}\left\{\dot{x}_{j0}^p\cdot e^{-i\omega t}\right\}$, and the pressure–radiation potential, ϕ_p^{qp}, around the device *q* due to unit time harmonic oscillating pressure head, $P_{in}^p=\mathrm{Re}\left\{p_{in0}^p\cdot e^{-i\omega t}\right\}$, in the chamber for the *p* device, i.e.

$$\phi^q\left(r_q,\theta_q,z\right)=\phi_D^q\left(r_q,\theta_q,z\right)+\sum_{p=1}^{N}\sum_{j=1}^{6}\dot{x}_{j0}^p\cdot\phi_j^{qp}\left(r_q,\theta_q,z\right)+\sum_{p=1}^{N}p_{in0}^p\cdot\phi_p^{qp}\left(r_q,\theta_q,z\right) \qquad (1)$$

These potentials ϕ_k^l ($l \equiv q$, qp ; k=D,1…,6, P; p=1, 2,…, N) are solutions of Laplace's equation in the entire fluid domain and satisfy the zero normal velocity on the sea bed $(z=0)$; the kinematic conditions on the q mean body's wetted surface and the boundary conditions at the outer and inner free sea surface of the q–th device $(z=d)$:

$$\omega^2\phi_k^l - g\,{}^{\partial\phi_k^l}\!/_{\partial Z} = \begin{cases} 0 & \text{for } r_q \ge a_q; \quad l \equiv q, k = D; \quad \text{or } l = qp, k = 1,2,...,6, P \\ 0 & \text{for } b_{1,q} \le r_q \le b_q; \quad l \equiv q, k = D; \quad \text{or } l = qp, k = 1,2,...,6 \\ -\delta_{q,p}\, i\omega/\rho & \text{for } b_{1,q} \le r_q \le b_q; \quad l \equiv qp; \quad k = P \end{cases} \tag{2}$$

The symbols that are used above are defined at Figure 1. The method for evaluating the fluid flow around the q device in the array relies on single device hydrodynamic characteristics and accounts for the hydrodynamic interactions among the devices using the physical idea of multiple scattering. Matched axisymmetric eigenfunction expansions in properly defined coaxial ring–shaped fluid regions around each body (see Fig. 1) have been used for evaluating the required single body hydrodynamic characteristics. In each fluid region appropriate series representations of the velocity potentials can be established, which must be continuous along with their first derivatives at the interfaces of neighboring fluid domains.

By the way of example, the wave field around the body q of the arrangement expressed in q–th device co–ordinate system is given by:

$$\phi_k^l(r_q,\theta_q,z) = \begin{cases} -i\omega\, {}^{H}\!/_{2} \sum_{m=-\infty}^{\infty} i^m \Psi_{k,m}^l(r_q,z)\cdot e^{im\theta_q}; & \text{for } k = D;\ l = q \\ -i\omega \sum_{m=-\infty}^{\infty} \Psi_{k,m}^l(r_q,z)\cdot e^{im\theta_q}; & \text{for } k = j;\ l = qp \\ {}^{1}\!/_{i\omega\rho} \sum_{m=-\infty}^{\infty} \Psi_{k,m}^l(r_q,z)\cdot e^{im\theta_q}; & \text{for } k = p;\ l = qp \end{cases} \tag{3}$$

For the inner fluid domain, in the q device's chamber, denoted by M (see. Fig. 1) the function $\Psi_{k,m}^l$ is given by:

$$\frac{1}{\delta_k}\Psi_{k,m}^l(r_q,z) = \delta_{q,p}\frac{1}{\delta_k}\Psi_{k,m}^q(r_q,z) + \sum_{j=0}^{\infty}\left(F_{k,m,j}^l R_{mj}^M(r_q) + F_{k,m,j}^{*l} R_{mj}^{*M}(r_q)\right)\cdot Z_j(z) \tag{4}$$

In Equation (4), $F_{k,m,j}^l$, $F_{k,m,j}^{*l}$, are the unknown Fourier coefficients for the velocity potential representation in the M field of the q device, the latter being considered open to the atmosphere and restrained and $Z_j(z) = \left\{0.5\left[1+\sin(2a_j d)/(2a_j d)\right]\right\}^{-1/2}\cos(a_j d)$. The term $\Psi_{k,m}^q$ is equal to:

$$\frac{1}{\delta_k}\Psi_{k,m}^q = \delta_{0,m} g_{k,m}^M(r_q,z) + p_{k,m}\sum_{j=0}^{\infty}\left(F_{k,m,j}^q R_{mj}^M(r_q) + F_{k,m,j}^{*q} R_{mj}^{*M}(r_q)\right)\cdot Z_j(z) \tag{5}$$

Here: $$g_{k,m}^M = \begin{cases} 0; & \text{for } k = D, j \\ 1; & \text{for } k = p \end{cases};\quad \delta_k = \begin{cases} d; & \text{for } k = D,\ j;\ j = 1,2,3 \\ d^2; & \text{for } k = j;\ j = 4,5,6 \\ 1; & \text{for } k = p \end{cases};\quad \text{and } p_{k,m} = \begin{cases} 0; & \text{for } k = D \\ 1; & \text{for } k = j \\ 1; & \text{for } k = p \text{ and } m = 0 \\ 0; & \text{for } k = p \text{ and } m \ne 0 \end{cases} \tag{6}$$

$$R_{mj}^M(r_q) = \frac{K_m(a_j b_{1,q})I_m(a_j r_q) - I_m(a_j b_{1,q})K_m(a_j r_q)}{I_m(a_j b_q)K_m(a_j b_{1,q}) - I_m(a_j b_{1,q})K_m(a_j b_q)};\quad R^{*M}{}_{mj}(r_q) = \frac{I_m(a_j b_q)K_m(a_j r_q) - K_m(a_j b_q)I_m(a_j r_q)}{I_m(a_j b_q)K_m(a_j b_{1,q}) - I_m(a_j b_{1,q})K_m(a_j b_q)} \tag{7}$$

where I_m, K_m, denotes the m–th order modified Bessel function of first and second kind, respectively. In Equation (5), $F_{k,m,j}^q$, $F_{k,m,j}^{*q}$ are the unknown Fourier coefficients for the device q in isolation condition.

3. Drift forces

By making use of the near–field method presented by Pinkster and Van Oortmerssen [2], the time–mean drift force and moment, acting on the device q of the array, can be obtained as:

$$F^{(2),q} = -\int_{WL}\frac{1}{2}\rho\cdot g\cdot\overline{\left(\zeta_r^q\right)^2}\,\mathrm{n}dl + \overline{M\cdot R}\cdot\overline{X_g^{q\,\prime\prime}} + \int\int_{S_0^q}\frac{1}{2}\cdot\rho\cdot\overline{\left|\nabla\Phi^q\right|^2}\,\mathrm{n}dS + \int\int_{S_0^q}\rho\cdot\overline{\overrightarrow{X^q}\cdot\nabla\Phi_t^q}\,\mathrm{n}dS \tag{8}$$

Here the bars denote the time average; S_0^q, is the mean q device's wetted surface; ρ is the water density; g is the gravity acceleration; $\mathbf{n}$ is the unit normal vector pointing outwards to the device; M is the generalized mass matrix; $\overrightarrow{X^q}$ is the vector of the first–order translations at a point on the device's wetted surface, which can be displaced as superposition of

translation motions of the bodies' center of gravity and the rotations around it. The term $\overrightarrow{X_g^q}$, is the first–order translational accelerations of body's center of gravity and ζ_r^q, is the first–order relative wave elevation with respect to the transposed static water line *WL* on the *q* device. In Eq. (8), generalized normal vector components and mass moments of inertia have to be considered for evaluating the mean drift moments.

Following the momentum conservation principle, the expressions for both horizontal and vertical mean drift forces and the corresponding moments are given by (Mavrakos, [11]):

$$F^{(2),q} = \rho \iint_{S_R} \left\{ \left[\Phi_t^q + \frac{1}{2}\nabla\Phi^q.\nabla\Phi^q + gz \right]\mathbf{n} - \frac{\partial\Phi^q}{\partial n}\nabla\Phi^q \right\} dS - \mathbf{k}\rho \iint_{S_B} \left[\Phi_t^q + \frac{1}{2}\nabla\Phi^q.\nabla\Phi^q \right] dS - \mathbf{k}\rho g \iint_{S_{FS}\cup S_0^q} zn_z dS \qquad (9)$$

$$M^{(2),q} = \rho \iint_{S_R} \left\{ \left[\Phi_t^q + \frac{1}{2}\nabla\Phi^q.\nabla\Phi^q + gz \right](\mathbf{x}\times\mathbf{n}) - (\mathbf{x}\times\nabla\Phi^q)\frac{\partial\Phi^q}{\partial n} \right\} dS - \rho \iint_{S_B} \left[\Phi_t^q + \frac{1}{2}\nabla\Phi^q.\nabla\Phi^q \right](y\mathbf{i} - x\mathbf{j}) dS - \rho g \iint_{S_{FS}\cup S_0^q} z\left[(yn_z - zn_y)\mathbf{i} + (zn_x - xn_z)\mathbf{j}\right] dS$$

Here, time averages over r.h.s of the above equations are understood, **k**, **i** and **j** are the unit vectors in z–, x– and y–axes respectively, **n** is the unit normal vector oriented outwards from the fluid control volume, **x** is the position vector of a point on the control surfaces with respect to the coordinate system of the examined device and the assumption was made that the sea bottom is horizontal. Moreover, S_B is the sea bottom, S_{FS} the portion of the free surface enclosed between S_0^q, and the fixed vertical cylindrical control surface S_R surrounding each OWC of the array, which in the present contribution it is assumed to coincide in the radial direction with the mean wetted surface of each device. The complete representation of the velocity potential around the OWC has to be taken into account by including both wave-like and evanescent wave modes (Mavrakos, [11]). Drift loads on the individual devices are properly superimposed with respect to a global co-ordinate system in order to evaluate the drift loads on the entire multi-body configuration considered as a unit.

3. Numerical results

In the present contribution results are plotted for three different configurations of OWC devices. In the first configuration we examined an array of three same OWC devices placed in a row, restrained in the wave impact. The devices are placed on the x axis of a Cartesian co–ordinate system and the wave angle with the y axis is $\theta = 0$. The radius and the draught of the concentric cylindrical body are $0.4m$; the radius and the draught of the oscillation chamber are $0.5m$ and the chamber's thickness is $0.1m$ (Figures 3,4). The water depth is equal to $5m$ and the distance between the vertical axis of

Fig. 3 Physical model of three OWC devices open to the atmosphere placed in a row

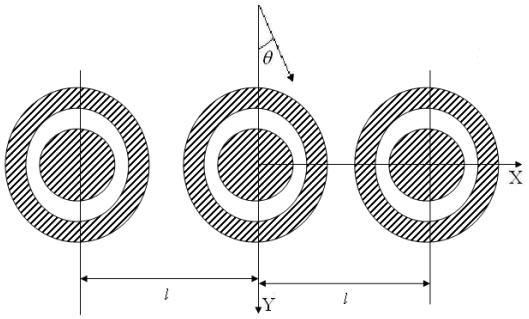

Fig. 4 Schematic representation of three OWC devices placed in a row

each device of the array is $2m$. The turbine parameter is either assumed, $\Lambda >> 0$, so the inner pressure in each device is equal to the atmospheric one (see [12]); or equal to an optimum coefficient of the same restrained OWC device but in isolation as in Evans and Porter [13] work. In the second configuration the above array of OWC devices is floating individually, and in the third configuration as a unit forming a platform. The mass and mass moment of inertia of each device were assumed equal to $0.254tn$, $0.062tn.m^2$, respectively; the mass and mass moment of inertia of the multi – device array were assumed equal to, $0.762tn$, $0.186tn.m^2$ respectively.

4. Acknowledgements

This research has been co-financed by the European Union (European Social Fund – ESF) and Greek national funds through the Operational Program "Education and Lifelong Learning" of the National Strategic Reference Framework (NSRF) 2007 – 2013: Research Funding Program: ARISTEIA, Program POSEIDON (2041)

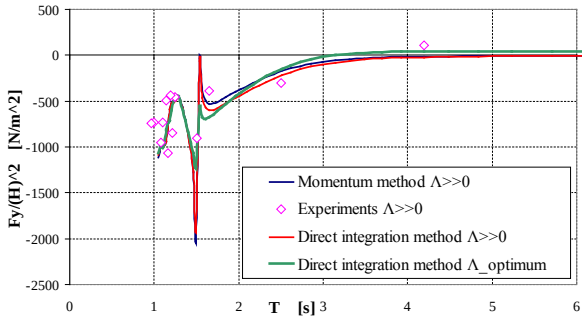

Fig. 5 Total horizontal drift force, on y axis, acting on the tail–end restrained devices of the array versus wave period.

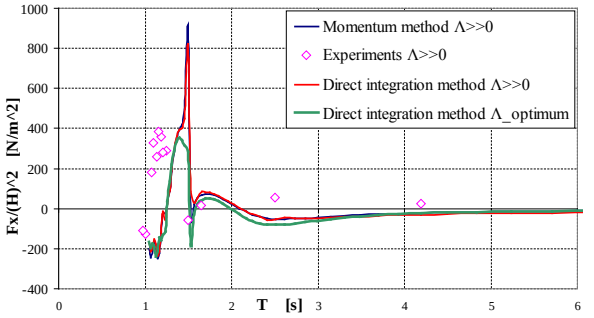

Fig. 6 Total horizontal drift force, on x axis, acting on the tail–end restrained devices of the array versus wave period.

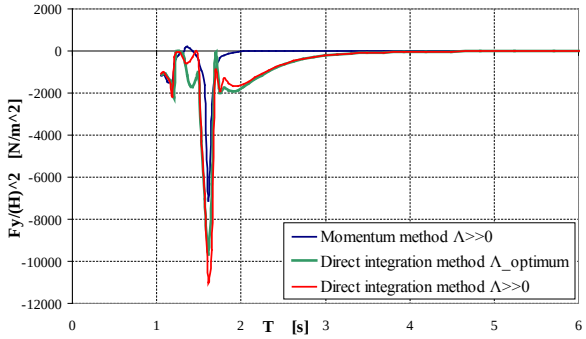

Fig. 7 Total horizontal drift force, on y axis, acting on the middle device of the floating individual array versus wave period.

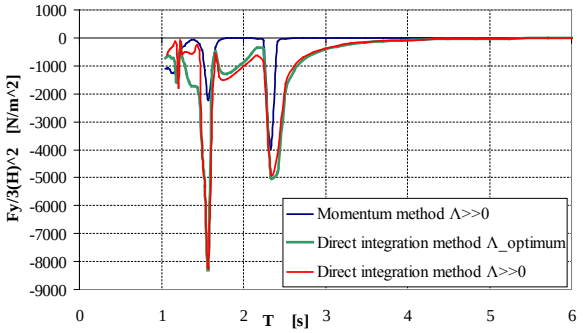

Fig. 8 Total horizontal drift force, on y axis, acting on the entire multi–device array system versus wave period.

5. References

[1] Konispoliatis, D., Mavrakos, S.A. 2013. Hydrodynamic interactions among multiple cylindrical OWC's devices restrained in regular waves. Proc. *28th International Workshop on Water Waves and Floating Bodies* (IWWWFB), L' Isle sur la Sorgue, pp. 113–116.

[2] Pinkster, J.A. and Oortmerssen, G.Van. 1977. Computation of the first and second order wave forces on oscillating bodies in regular waves. Proc. *2nd Int. Conf. on Numerical Ship Hydrodynamics*, Berkeley.

[3] Hong D.C. et al. 2004. Numerical study of the motions and drift force of a floating OWC device. *Ocean Engineering* **31**, pp. 139–164.

[4] Maruo, H. 1960. The drift of a body floating in waves. *J. Ship. Res.* **4**, pp. 1–10.

[5] Newman, J.N. 1967. The drift force and moment on ships in waves. *J. Ship. Res.* Vol. **11**, 1, pp. 51–60.

[6] Faltinsen, O.M. and Michelsen, F.C. 1974. Motions of large structures in waves at zero Froude number. Proc. *Int. Symp. on Dynamics of Marine Vehicles and Structures in Waves*, Univ. Coll. London, pp. 91–106.

[7] Molin, B. 1983. On second-order motion and vertical drift forces for three-dimensional bodies in regular waves. Proc. *Int.Workshop on Ship and Platform Motion*, Berkeley, pp 344–357.

[8] Twersky, V. 1952. Multiple scattering of radiation by an arbitrary configuration of parallel cylinders. *J. Acoustical Soc. of America*, **24** (1).

[9] Mavrakos, S.A. 1991. Hydrodynamic coefficients for groups of interacting vertical axisymmetric bodies, *Ocean Engineering*, **18**(5), pp. 485 – 515.

[10] Mavrakos, S.A., Chatjigeorgiou, I.K., Mazarakos, T.P., Konispoliatis, D.N., Maron, A. 2011. Hydrodynamic forces and wave run–up on concentric cylinders forming piston like arrangements. Proc. *26th International Workshop on Water Waves and Floating Bodies* (IWWWFB 2011), Athens, pp. 109–112.

[11] Mavrakos, S.A., "Mean drift loads on multiple vertical axisymmetric bodies in regular waves", Proceedings, *5th International Offshore and Polar Engineering Conference (ISOPE'95)*, The Hagen, The Netherlands, 1995, Vol. **3**, 547-555.

[12] Mavrakos, S. A., Konispoliatis, D.N. 2012. Hydrodynamic analysis of a vertical axisymmetric oscillating water column device floating in finite depth waters. Proc. *31st International Conference on Ocean, Offshore and Arctic Engineering* (OMAE 2012), Rio de Janeiro, Brazil.

[13] Evans, D.V., Porter, R. 1997. Efficient calculation of hydrodynamic properties of OWC-type devices. *Journal of Offshore Mechanics and Arctic Engineering*, Vol. 119, No. **4**, pp. 210–218.